THE BOEING COMPANY
Aerospace Group

IDENTIFYING OPTIMUM PARAMETERS OF HOT EXTRUSIONS

Contract NAS 7-276

Prepared for

Chief, Materials Research Branch
National Aeronautics & Space Administration
Headquarters
Washington, D.C.

Progress Report No. 15
18 October, 1967 to 11 January, 1968

THE BOEING COMPANY
Aerospace Group

IDENTIFYING OPTIMUM PARAMETERS OF HOT EXTRUSIONS

Contract NAS 7-276

Prepared for

Chief, Materials Research Branch
National Aeronautics & Space Administration
Headquarters
Washington, D.C.

Progress Report No. 15
18 October, 1967 to 11 January, 1968

ABSTRACT

Six extrusions were attempted during this period, three of which were successfully extruded. One successful and one stalled extrusion having MgO powder "insulation" showed that low (less than 20% dense) powder densities led to non-uniformities. However, results indicate that the "insulation" lowers the heating required for extrusion and reduces the resultant grain size. Analyses also indicate that forging of specimens prior to extrusion reduces grain size.

It is confirmed that ZrO_2 and CaO are extrudable at lower temperatures than MgO, and that ZrO_2 also rapidly recrystallizes. Additives to ZrO_2, such as CaO, appear to speed recrystallization and slow decomposition.

Extruded MgO crystals show a "pseudo-crystal" texture. Extruded ZrO_2 appears to have a $\langle 100 \rangle$ axial texture (like that of MgO and CaO) which is destroyed by recrystallization and grain growth.

Use of steel shells on the outside of extrusions appears promising to reduce the volume of refractory metal and allow better lubrication. However, graphite cannot replace the refractory metal.

CONTENTS

LIST OF FIGURES

WORK ACCOMPLISHED

I. EXTRUSION

A. Purpose and Parameters

Six extrusions were attempted in this reporting period. One was the extrusion of 1" square ceramic bodies in an insulating can like that shown in Figure 1. Billets of square cross section were again used because such a shape was much easier to obtain in many of the specimens desired to be extruded. MgO powder was used for the "insulation", but its packing was very poor, giving an estimated loaded density of less than 20% of theoretical density.

This extrusion was instrumented with two W-5 Re/W-26 Re thermocouples insulated with BeO and sheathed in molybdenum. These were located approximately half way toward the front of the can along the 2.46" ID can bore. This extrusion (MgO-26) was heated to approximately 2000°C (average thermocouple readings) and successfully extruded despite some delay in loading the billet in the press. Extrusion parameters and billet data are shown in Tables I and II.

The other metal can extrusion (MgO-25) was planned to further investigate the effects of higher reduction ratios. It had MgO powder insulation between the 1.5 and 2.0" diameter MgO billets (wrapped in W foil) and the 2.46" ID bore of the TZM can and was similarly instrumented with thermocouples. The powder "insulation" was put in the can as a slurry of MgO + ethanol, which improved packing some, but still left its density quite low after drying. Some problem of fogging of the sight glass was observed, and one thermocouple behaved erratically, so its lower reading was neglected in determining the dropping of the billet. There was also a delay in loading of this can, and the press stalled without any extrusion. Parameters and billet data are given in Tables I and II.

In order to investigate fluid extrusion of ceramics, some inexpensive, small scale, experiments were planned on a smaller press to develop some of the necessary design parameters and handling techniques (e.g., how to assure proper alignment of the ceramic billet with the die and sealing of the die by the billet so adequate "fluid" pressure is developed). The first two trials used steel billets and heat treating salt for the "fluid" (melting point $\sim$ 570°C). The latter was melted into the space between the billets and the steel container, then the container was welded shut. Bloating of the cans on re-heating for extrusion prevented their successful extrusion.

The last two extrusions had two purposes. The first purpose was to see if a steel shell could be used on the outside of metal cans to reduce the volume of expensive refractory metal and allow the use of better lubrication as is done in some other extrusion processes. The second purpose was to see if graphite could be used for canning in place of the refractory metal. Such a replacement is suggested by the use of graphite as a removable core material for extrusion of metal tubes. These steel-graphite cans were constructed as shown in Figure 2, except the second one used a 0.25" thick steel wall (the same graphite wall thickness was used by making the ID of the graphite can smaller). These were also instrumented with thermocouples and were assembled in the press. The steel components were heated separately as shown in Figure 2. The heating of the graphite can with MgO billets and subsequent extrusion parameters are shown in Table I.

B. Extrusion Description

The thin wall (0.120") steel shell of the first steel-graphite can extrusion broke into several short fragments on extrusion. The graphite component disintegrated. The MgO billets were fragmented but indicated only limited, inhomogeneous reduction in cross section. The thicker steel shell of the second of these extrusions broke in only one place on extrusion, but the graphite and MgO behaved similar to the first such extrusion.

The billets of the stalled high reduction extrusion (MgO-25) had expanded radially and non-uniformly. The 1.5" diameter billets approached 2" in diameter consolidating the surrounding MgO powder.

The insulating can broke in three places and developed several tears in the TZM can as shown by the two main sections of Figure 3A. The can was warped, and there was additional minor warping of the ceramic inside of the can due to billets "wandering" in the low density MgO insulating layers. The forged MgO (see Figure 3B) and CaO, and part of the ZrO_2 billets were fairly uniform but the MgO crystal, hot pressed MgO billets, and part of the ZrO_2 did not retain a uniform square cross section. The Al_2O_3 billets were very non-uniform, and did not show as much reduction as the rest of the billets. The can was removed from most of the ZrO_2, forged CaO, forged MgO, and MgO crystal billets. The two MgO billets showed incomplete transverse cracking progressing from the outside inward (e.g. Figure 3B), but the ZrO_2 and CaO did not. Transverse cracking was most severe in the MgO crystal. Little other cracking was found in the forged MgO crystal billet; however, the two ZrO_2 billets had many fine, random cracks. The ZrO_2 (partially stabilized with CaO) retained its light yellow color, but the other ZrO_2 (Zircoa 1027) had turned a medium brown color. Most of the forged MgO crystal had clouded so it was only translucent, and the cloudy forged CaO appeared to have clouded some more, while the MgO crystal remained transparent.

Part of the can around the forged CaO billet (CcF-1-4) was cut open. The billet sections were easily removed, indicating little or no bonding which had been observed in earlier extrusions using hot pressed billets.

II. MATERIAL ANALYSIS

A. Microstructure

Grain size data for stalled extrusions are shown in Table III. Data on extruded grain sizes in extrusion MgO-26 (insulating can) are shown in Table II, and microstructure of some of these bodies is shown in Figures 4 - 6. The ZrO_2 partially stabilized with CaO (Figure 4) showed some signs of remnant elongated grains which have an internal structure. However, the grain size was mixed, with the percent of finer grain increasing toward the surface. The Zircoa 1027 ZrO_2 (Figure 5) showed more pronounced grain elongation with more uniform microstructure. For comparative purposes, microstructure of two earlier higher temperature extrusions of ZrO_2 are shown in Figures 6 and 7, and comparative grain sizes are shown in Table IV, indicating that the ZrO_2 partially stabilized with CaO has a finer grain size and this increases with extrusion temperature.

The forged CaO billet (CcF-1-4) also showed some remnant grain elongation (Figure 8) which is also reflected in the grain size data of Table II.

The forged MgO billet (McF-1-13) showed some variation in grain size. Two sample transverse sections showed average grain sizes of 19 and 29 microns, while one longitudinal section showed a grain size of 89 microns. Some possible residual grain elongation was left. The difference in transverse and longitudinal grain sizes of Table II reflects some of this, but it also reflects grain size variation.

Fracturing of the two ZrO_2 billets (Z-1-5, Figure 4; Z-2-1, Figure 5) was often along boundaries of the elongated grains. Electron probe analysis of Z-1-5, Z-2-1, and Z-1-1, showed no second phase accumulation along grain boundaries or fractures as had been found in the darkened, higher temperature ZrO_2 extrusion of Z-1-3.

B. Strength

Two specimens for strength testing were obtained from McF-1-13; one fractured at 37.5×10^3 psi, and the other at 29.0×10^3 psi. (Grain sizes were respectively 19 and 29 microns). The former failed from the corner which was missing a chip suggesting a flaw, and the second clearly failed from a flaw.

C. Orientation

A number of extruded samples were examined by x-ray diffraction with an improved automatic pole figure plotter* based on that reported by R. M. Eichhorn (Rev. Sci. Instr. 36 (7), pp 997-1000, July 1965). The instrument plots orientation data from transverse and longitudinal sections separately. A complete pole figure is made by estimating the cross sectional profile of the transverse data (which is plotted as a plane projection of the transverse section), and making a composite of this with the longitudinal data. While not giving as much detail, it allows examination of many more samples since 3 or 4 specimens can be run in a day instead of 1 every 2 or 3 days. Improved standards, approaching the density and grain size of extruded bodies were also made. All specimens were examined with CuKα radiation.

This showed the same general (200) pole figure for extruded hot pressed MgO having concentrations at the "north and south poles" and in an "equitorial band" (e.g. Figure 9). Examination of several fused MgO extrusions showed that they had similar pole figures except that instead of a complete band across the "equator", they had one to three concentrations of poles (e.g. Figures 10 - 12). Examination of McF-1-13, the forged MgO crystal extrusion, showed a pattern similar to that of Figure 9.

The forged CaO billet (CcF-1-4) also showed a pattern (Figure 13) more like an extruded polycrystalline body than an extruded crystal. The intensity of the (200) poles of the CaO were less than those of MgO in agreement with earlier work on extruded CaO using hot pressed bodies.

The improved standards showed that intensities of oriented lines were not as great as previously reported. Peak intensities sometimes ran over 20 times random, instead of 200 times, and oriented intensities were about 4 times intensities for a random sample over a reasonable area instead of about 40.

Sample testing of extruded ZrO_2 showed possible signs of a $\langle 100 \rangle$ axial texture, especially in the lowest temperature extrusion (MgO-26). However, this was only at most about 1.3 times a random standard.

*Designed by R. Racus of the Boeing Metallurgical Laboratory, Aerospace Group, Space Division.

DISCUSSION AND CONCLUSIONS

I. EXTRUSION

The "wandering" of the ceramic billets in the insulating can and the non-uniform radial upsetting (expansion) of the intended high reduction billets shows that the low density of the MgO powder insulation was inadequate. The steel shell on the outside of the steel-graphite can extrusions shows promise, but the graphite was completely inadequate. With a molybdenum or TZM can, the thinner steel shell may also work well. The bloating of the steel container by the heat treating salt indicates that the containers should not be sealed, or else, the bloating problem must be solved (e.g. outgassing or allowing more room for expansion).

The stalling of the planned high reduction extrusion is probably due at least partially to the delay in loading in the press. However, the grain size (Table III) indicates less heating than the one "normally operating" thermocouple indicated, unless the limited upsetting reduced grain size. From forging experience, the amount of deformation seems inadequate for this.

The incomplete fracturing of the fused MgO billets (M-f-15, McF-1-13) in extrusion MgO-26 is the beginning of wafering. Complete and more extensive wafering was observed in previous extrusions dropped at an optical pyrometer reading of 2000°C or lower at the rear of the can. This reduced wafering at the same or lower temperature, with some delay in loading, indicates that the insulating can limited heat losses as expected. The similar, but apparently slightly smaller, grain size in this and the earlier extrusion of ZrO_2 (partially stabilized with CaO) at 2000°C indicates that the thermocouples show temperatures fairly close to those read optically at the rear of earlier cans. This is consistent with previous observations that such earlier, shorter cans were heated more uniformly.

The extrusion of the CaO and ZrO_2 without wafering confirms that they are extrudable at lower temperatures than MgO. The elongated grains in the ZrO_2 and the lack of second phase accumulation at grain boundaries indicates that this is due to true deformation and not impurity enhanced grain boundary sliding. The apparent lack of bonding of the CaO to the TZM can indicates that previous bonding may have been due to impurities found in hot pressed bodies used earlier.

II. ANALYSIS

The 30 micron grain size of billet M-6-14 of extrusion MgO-26 is smaller than average, especially for a billet previously fired to 1540°C. This, along with the apparently slightly smaller grain size of the ZrO_2, corroborates the lower extrusion temperature indicated by the thermocouple. This also indicates that the insulating can concept is valid.

The pole figures of extruded MgO crystals show that they have about the same ⟨100⟩ axial texture as that from hot pressed billets. However, they lack the random orientation about the extrusion axis since they do not have complete "equitorial" bands. The "equitorial patches" are about 90° apart. Thus only one patch may show if it is at the center (0° from the normal) since sensitivity drops rapidly above 75° to the normal so the other two at ±90° would not be detected. If these patches are not centered at 0° due to the orientation of the plane selected for examination, then two patches should appear as in Figure 11. If one or more patches are larger, then one complete and two incomplete patches may be seen as in Figure 12. These patches at about 90° intervals represent a pseudo, but fairly distorted ⟨100⟩ crystal orientation perpendicular to the axis, that is concentration of ⟨100⟩ poles in two perpendicular directions similar to a distorted single crystal with two of its six ⟨100⟩ faces perpendicular to the extrusion axis. This additional texturing in two perpendicular radial directions would further reduce average grain boundary misorientations. This may raise strengths of such specimens above that of specimens with random orientations about the axis. The fact that the pole figure for the forged-extruded crystals is like that for hot pressed bodies indicates that forging has altered the crystals and their resulting structure.

After extrusion, the grain size of the forged MgO crystal was much smaller than that of the unforged crystal, indicating substantial advantage of forging prior to extrusion as predicted. This advantage is further indicated by noting that a grain size of 19 microns was observed in one specimen of the forged-extruded crystal, which is slightly less than the finest extruded grain size from a hot pressed billet (20 microns), and more clearly below the finest grain size observed in a single crystal extrusion (29 microns). However, more data must be obtained to make sure that these are not just unusual variations independent of forging. Also, since this billet clouded, it must be ascertained that the finer grain size was not due to some impurity effect. Nonetheless, the reduction in grain size is encouraging.

The ZrO_2 microstructures clearly suggest grain elongation and subsequent recrystallization as has been found for MgO and CaO. The lack of detectable elongated regions in higher temperature extrusions (e.g. Figure 7) is apparently due to grain growth, which is shown in Table IV. Comparison of ZrO_2 billets Z-1-5 and Z-2-1 shows that stabilizing agents may effect recrystallization. The observation of very low texturing in the lowest temperature extrusion, and none in the highest temperature extrusion indicates that recrystallization destroys the texture of extruded ZrO_2.

The brown color of the Zircoa 1027 ZrO_2 suggests some loss of oxygen. The lack of this in the ZrO_2 with CaO indicates that stabilizing agents may also help stabilize the stoichiometry of ZrO_2. No grain boundary accumulation of CaO was observed in the lower temperature ($\sim$ 2000°C) un-discolored extrusion. However, such accumulation was found in the earlier, higher temperature (2200°C)

extrusion, where the ZrO_2 was discolored to a brown inside and a black color on the surface. This suggests that phase separation and loss of oxygen are related.

The lower reduction of the alumina and spinel billets in extrusion MgO-26, and their greater non-unfiromity indicates poor extrudability at normal strain rates as previously observed.

III. SUMMARY

Analysis indicates that the insulating can limits extrusion heating and resultant grain size as predicted. However, further conformation is desired, and dense insulating layers are needed. Forging also appears to reduce grain size, but again further conformation is required to rule out statistical variations and impurity effects (as indicated by clouding).

Extruded single crystals have a pseudo-single crystal texture after extrusion rather than a random orientation of $\{100\}$ plane parallel with the extrusion axis as found for extruded hot pressed bodies. Forged-extruded crystals have a texture like that of extruded hot pressed bodies.

Extruded ZrO_2 shows grain elongation with recrystallization similar to MgO and CaO. Higher temperatures eliminate traces of this elongation, apparently due to grain growth after recrystallization. These processes of recrystallization and grain growth appear to destroy an apparent $\langle 100 \rangle$ axial extrusion texture. Agents to stabilize the cubic structure in ZrO_2 also appear to aid recrystallization and inhibit decomposition (as suggested by darkening of the bodies).

It is confirmed that both ZrO_2 and CaO are extrudable at lower temperatures than MgO.

Graphite cannot replace the refractory metal can in extrusion. However, use of an outer steel shell to allow use of better lubrication and reduce the volume of refractory metal can appears feasible for MgO, as it was for UO_2 (see Hunt and Lowenstein, Am. Ceram. Bul. 43 (8), pp 562-65, 1964).

FUTURE WORK

Investigation of insulating can extrusions will be continued. Different, denser forms of MgO "insulation" will be used. Further study of extrusion of forged bodies will also be carried out. Evaluation of fluid extrusion techniques and parameters will also be continued.

TABLE I EXTRUSION PARAMETERS

Extrusion	Can Material	Can O.D. (in)	Ceramic Billet Diameter (in)	Heated to °C (1)	Area Reduction Ratio	Ram Speed (in/sec)	Pressure (tons/in^2) Upset	Pressure (tons/in^2) Running
MgO-25 (High Reduction)	TZM	3.0	1.5-2.0	1850(2260)	16 to 1	-(2)	108	-(2)
MgO-26 (Insulating Can)	TZM, MgO Powder (see Figure 1)	3.0	1.0(3)	1800(2000)	9 to 1	13	103	76
MgO-27	Steel, Graphite, MgO Powder (see Figure 2)	3.0	1.0	1880	9 to 1	9	76	62
MgO-28		3.0	1.0	1830(1920)	9 to 1	10	83	62

(1) Temperature on dropping from furnace, first figure shown is optical pyrometer reading on the tail of the billet, figure in parentheses is the reading of 1 or 2 W-5 Re/W-26 Re thermocouples located inside of the can, about half way between the front and rear.

(2) Extrusion stalled.

(3) Billets 1" square in cross section.

TABLE II. EXTRUDED BILLET DATA

Number[1]	Composition	Fabrication[2]	Density (gm/cc) Before Extrusion[3]	Density (gm/cc) After Extrusion[4]	Area Reduction Ratio	Average Grain Size (microns) Transverse	Average Grain Size (microns) Longitudinal
Extrusion Number MgO-25: Stalled, apparently due to excessive cooling during loading.							
M-5-3	MgO	B	3.52				
M-4-25			3.58				
M-6-12			3.57				
M-4-18							
M-6-3			3.55				
M-5-18			3.57				
M-5-1			3.58				
M5N-1-11	MgO+5 w/o NiO		3.67				
M-f-8	MgO	Fusion					
Extrusion Number MgO-26 (Insulating Can), Drop Temperature: 1830°C(2000°C)[5], Reduction Ratio: 9 to 1							
C-f-1	CaO	Fused					
CcF-1-4	CaO	Fused, Forged			~9 to 1	142	211
M-f-15	MgO	Fused	3.58	3.58		100	
McF-1-13	MgO	Fused, Forged	3.58	3.58	~9 to 1	24	40
M-6-14	MgO	B				30	
Z-2-1	ZrO_2	Sintered[6]			~9 to 1	25	(160)[7] 27
Z-1-5	ZrO_2 (2.9% CaO)					16	(60)[7] 20
S_{ma}-1-8	$MgAl_2O_4$	B	3.42				
A-1-9	Al_2O_3	B	3.13				
A-1-16	$Al_2O_3 + Cr_2O_3$	Ruby Crystal					

(1) Billets listed from front to rear of the can.
(2) B refers to Vacuum Hot Pressing Procedure B or modifications thereof.
(3) Average error estimated at ±0.001 gm/cc.
(4) Average error estimated at ±0.02 gm/cc. Note: cracking will reduce apparent density.
(5) Optical pryometer temperature at the rear of the can (thermocouple reading in the can).
(6) These two billets were side by side.
(7) Grain sizes in parentheses are the estimated elongated grain size before recrystallization.

TABLE III - BILLET GRAIN SIZE AFTER HEATING FOR EXTRUSION

Billet	Billet Firing °C	Extrusion Heating °C[1]	Dia. (in)	Density, gm/cc Before Heating	Density, gm/cc After Heating	Final Grain Size (microns)	
M-1-8 (LiF)*	1565	2200	1.5	3.53	3.58	163	
M5N-1-1 (LiF)	1565	"	"	3.27		100	Extrusion MgO-7
M1A-1-9 (LiF)	1380	"	"	3.50		400	
M-2-20	1315	"	"	3.59		76	
M-3-1	1315	"	"	3.54		65	
M-3-2	1315	"	"	3.56		50	
M-2-7	1565	"	"	3.59		90	Extrusion MgO-10
M-2-21	1315	"	"	3.58		64	
m-1-1	-	"	"	1.5		38	
OP-211	-	"	0.75	3.58	3.58+[3]	Outside 3000 Center (98)	
M-3-25	1205	"(2)	1.0	3.38	3.39	38	
M-3-17	1315	"(2)	1.5	3.52	3.53	33	
M-3-13	1205	"(2)	1.5	3.56		70	Extrusion MgO-16
M-3-21	1205	"(2)	1.5	3.31	3.35	36	
M-3-24 (LiF)	1205	"(2)	1.5	3.27		56	

TABLE III - CONTINUED

Billet	Billet Firing °C	Extrusion Heating °C[1]	Dia. (in)	Density, gm/cc Before Heating	Density, gm/cc After Heating	Final Grain Size (microns)	
M-3-11	1315	2200	1.0	3.59	3.58+[3]	191	
M-3-22	1205	"	1.0	3.60	3.58+[3]	185	
M-3-16	1315	"	1.5	3.59	3.58+[3]	507	Extrusion MgO-17
M-3-20	1205	"	1.5	3.58	3.58+[3]	160	
M-3-6	1315	"	2.0	3.58	3.58+[3]	162	
m-1-4	-	"	0.9	1.5	3.56	55	
M-1-17	1565	"(2)	1.5	3.54	3.58+[3]	133	
M-3-12	1315	"(2)	1.5	3.58		102	
M2N-1-4	1565	"(2)	1.5	3.47	3.49	100	
M5N-1-3	1565	"(2)	1.5	-	3.41	58	Extrusion MgO-20
M1A-1-5	1315	"(2)	1.5	3.55	3.55	107	
M5A-1-3	1565	"(2)	1.5	3.43		40	
M2C-1-1	1315	2350[4]	1.5	3.57		188	
M1C-1-1	1315	2350	1.5	3.58		220	Extrusion MgO-23
MZ/2-1-1	1315	2350	1.5	3.55		301	
M5A-1-4	1315	2350	1.5	3.52		209	

TABLE III - CONTINUED

Billet	Billet Firing °C	Extrusion Heating °C[1]	Dia. (in)	Density, gm/cc Before Heating	Density, gm/cc After Heating	Final Grain Size (microns)	
M-5-3	1540	1810 (2260, 1850)[5]	1.5	3.52	3.55	87.4	
M-4-25	1540	"	1.5	3.58	3.58[6]	31.2	
M-6-12	1540	"	2.0	3.57	3.55	41.0	
M-4-18	1455	"	2.0		3.58	74.2	Extrusion MgO-25
M-6-3	1595	"	2.0	3.55	3.55	29.0	
M-5-18	1595	"	1.5	3.57	3.54	107	
M-5-1	1595	"	1.5	3.58	3.53	105	
M5N-1-11	1565	"	1.5	3.67	3.60	129	

*(LiF) means the billet was hot pressed with 2 w/o LiF.

(1) Optical reading at rear of can just before dropping billet.

(2) Central area of TZM shell melted indicating temperatures above 2200°C.

(3) Estimated near theoretical density from translucency.

(4) Central area of the ZrO_2 furnace liner apparently melted.

(5) Readings of W-5 Re/W-26 Re thermocouples in the can.

(6) Some density figures are low due to fracturing.

TABLE IV. EXTRUDED ZrO_2 GRAIN SIZES

Billet	Extrusion	Heated to °C(1)	Grain Size (microns) Transverse	Longitudinal
Z-2-1	MgO-26	1830	25	27
Z-1-5	MgO-26	1830	16	20
Z-1-1	MC-1	2000	17	21
Z-1-3	MgO-12	2200	32	39

(1) Optical pyrometer reading at the rear of the billet just prior to dropping for loading in the press.

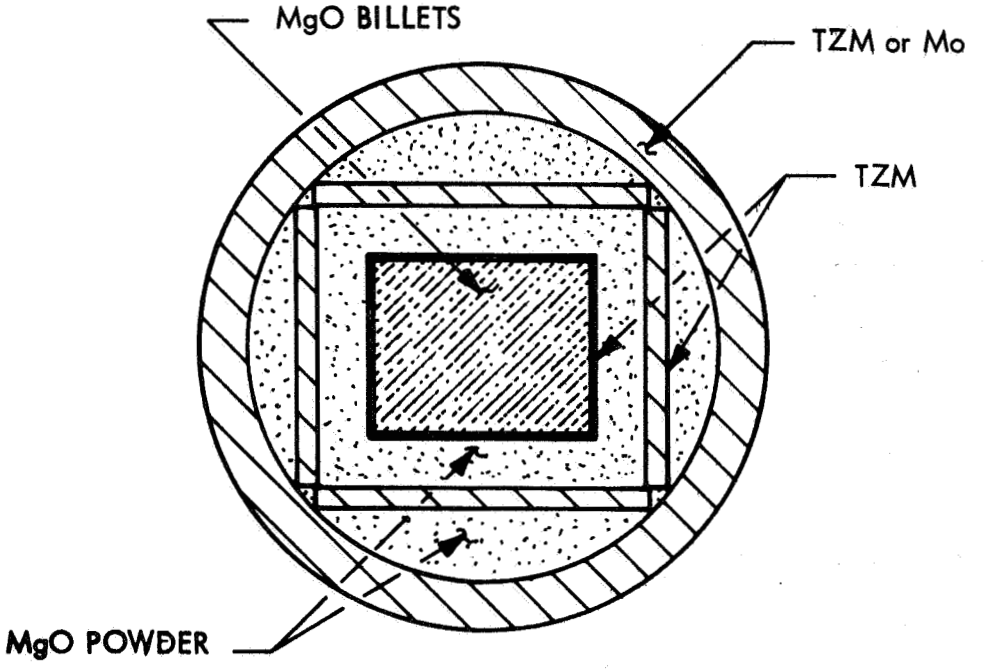

FIGURE 1. INSULATING CAN USING SQUARE INTERNAL SECTIONS

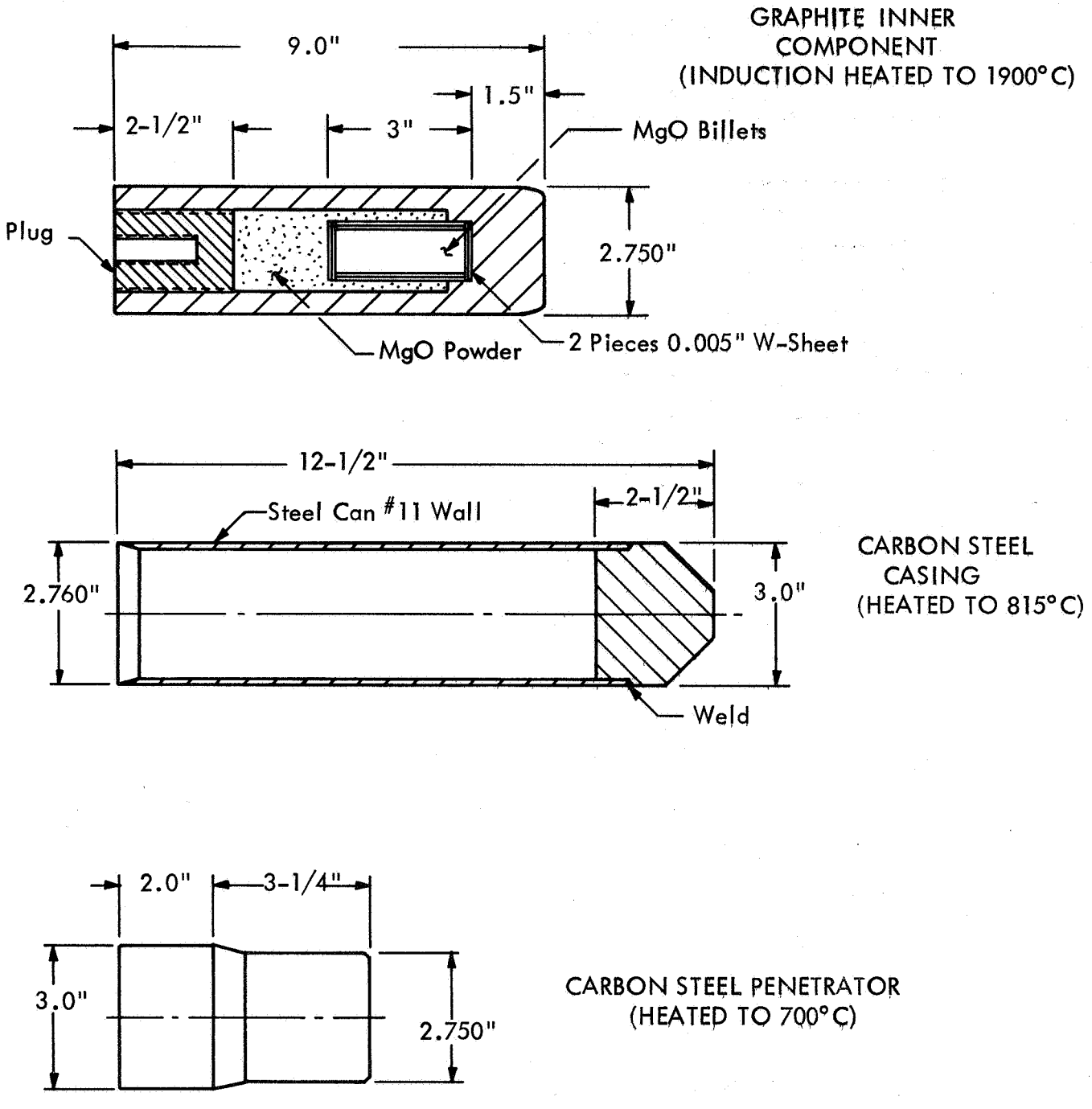

FIGURE 2. GRAPHITE-STEEL EXTRUSION CAN

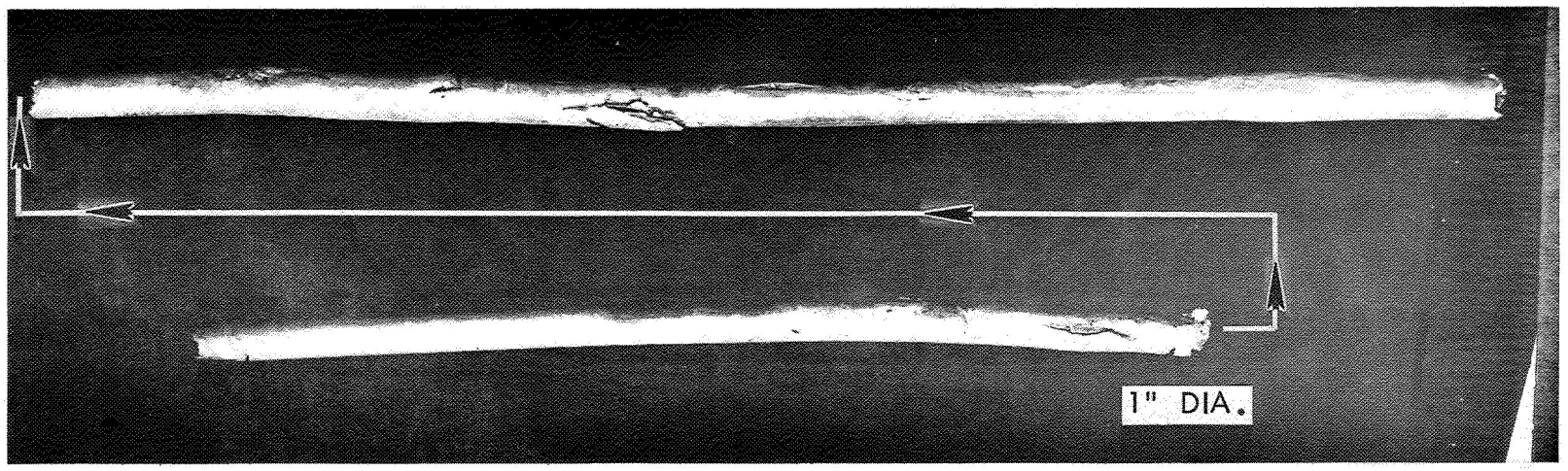

A

EXTRUSION DIRECTION ⟶

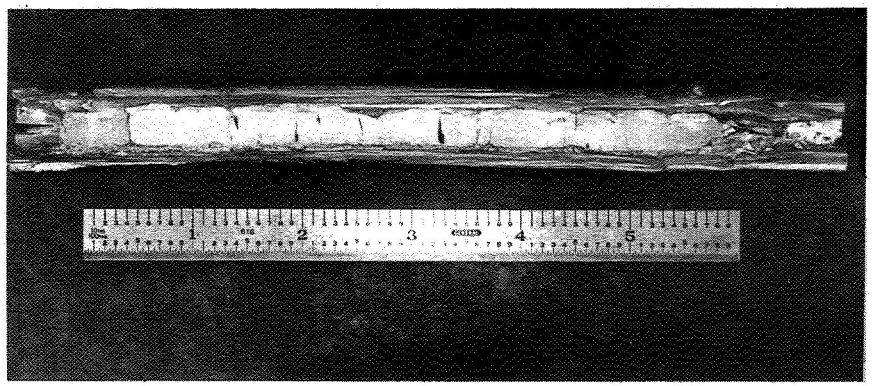

B

FIGURE 3 EXTRUSION MgO-26. INSULATING CAN EXTRUSION USING MgO POWDER "INSULATION". (A) TWO MAIN SECTIONS AS EXTRUDED. NOTE TEARS IN THE OUTER METAL SHELL. (B) PHOTO OF BILLET McF-1-13 (FORGED MgO CRYSTAL) WITH MOST OF THE CAN REMOVED. THIS WAS THE MOST UNIFORM BILLET IN THE EXTRUSION.

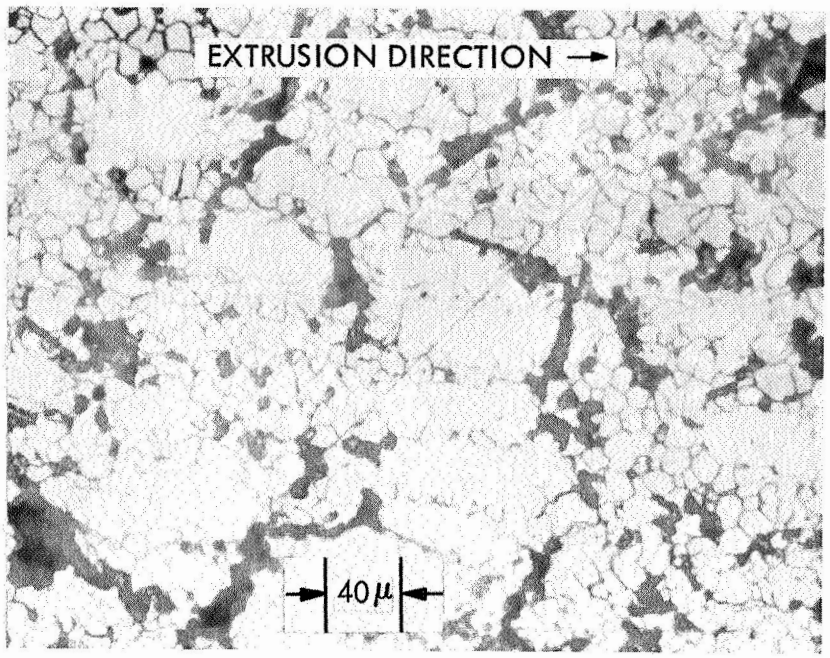

A

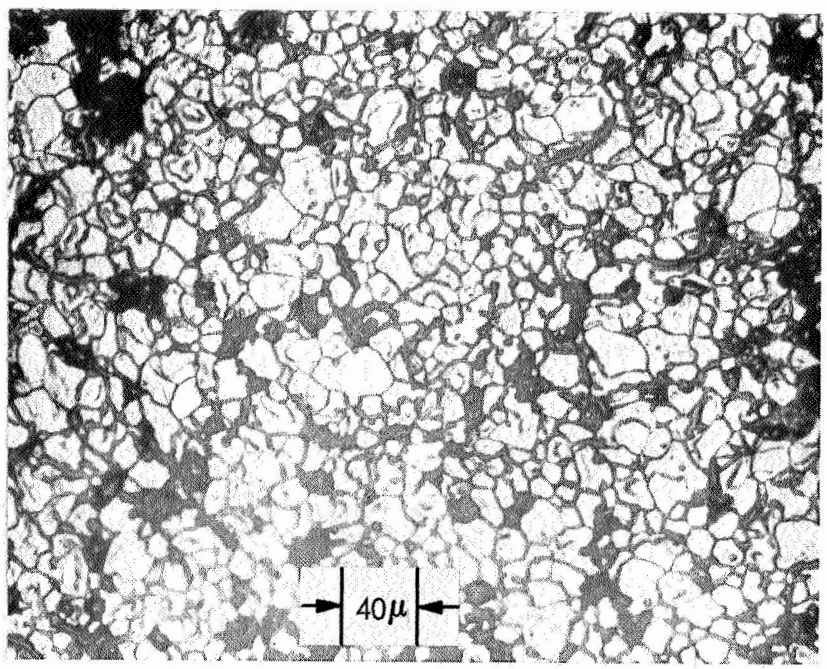

B

FIGURE 4 EXTRUDED ZrO_2 MICROSTRUCTURE. MATERIAL ZIRCOA-C, PARTIALLY STABILIZED WITH 2.9% CaO. BILLET Z-1-5, EXTRUSION MgO-26, HEATED TO APPROXIMATELY 2000°C (THERMOCOUPLE READING, OPTICAL PYROMETER READING WAS ABOUT 1830°C). (A) LONGITUDINAL, (B) TRANSVERSE SECTION. ETCHED APPROXIMATELY 5 MINUTES IN BOILING H_3PO_4. NOTE MIXED GRAIN STRUCTURE. THE NUMBER OF FINER GRAINS INCREASED TOWARD THE SURFACE OF THE EXTRUSION. THESE SECTIONS ARE NEAR THE SURFACE.

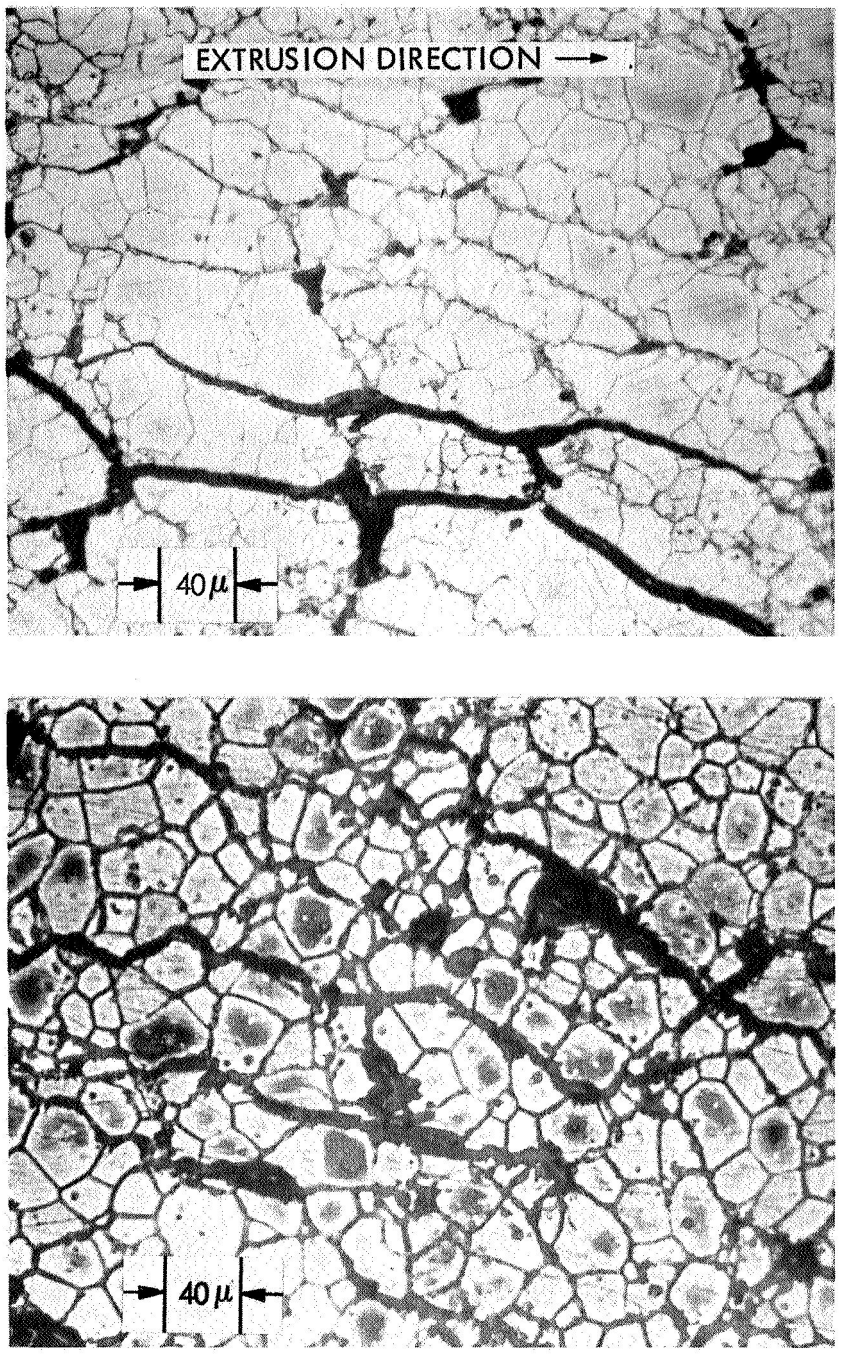

FIGURE 5 EXTRUDED ZrO_2 MICROSTRUCTURE. MATERIAL ZIRCOA 1027. BILLET Z-2-1, EXTRUSION MgO-26, HEATED TO APPROXIMATELY 2000°C (THERMOCOUPLE READING, OPTICAL PYROMETER READING WAS ABOUT 1830°C). (A) LONGITUDINAL, (B) TRANSVERSE SECTION. BOTH ETCHED IN BOILING H_3PO_4. NOTE SUBSTANTIAL INTERGRANULAR CRACKING.

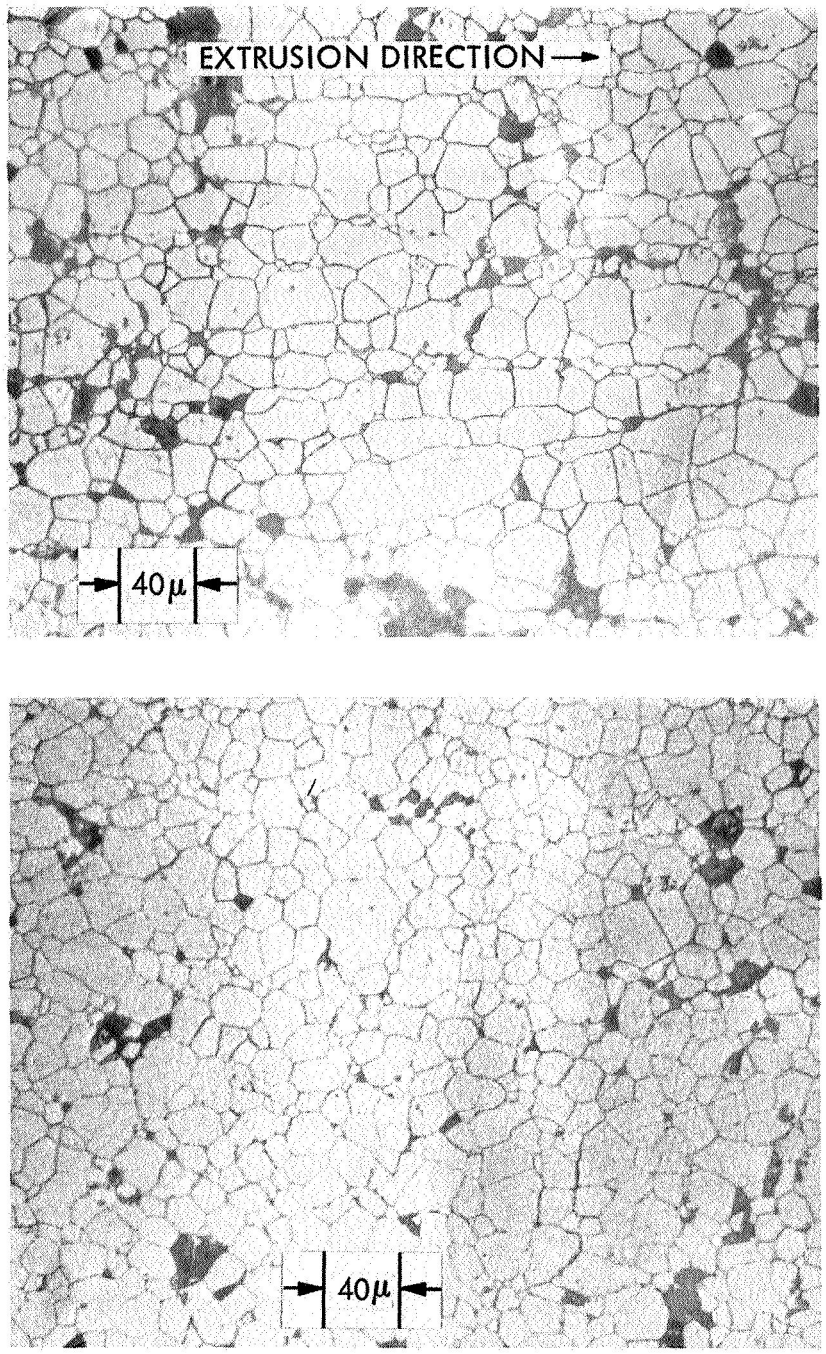

FIGURE 6 EXTRUDED ZrO_2 MICROSTRUCTURE. MATERIAL ZIRCOA C, PARTIALLY STABILIZED WITH 2.9% CaO. BILLET Z-1-1, EXTRUSION MC-1 HEATED TO APPROXIMATELY 2000°C (OPTICAL PYROMETER READING). (A) LONGITUDINAL, (B) TRANSVERSE SECTIONS. ETCHED IN BOILING H_3PO_4.

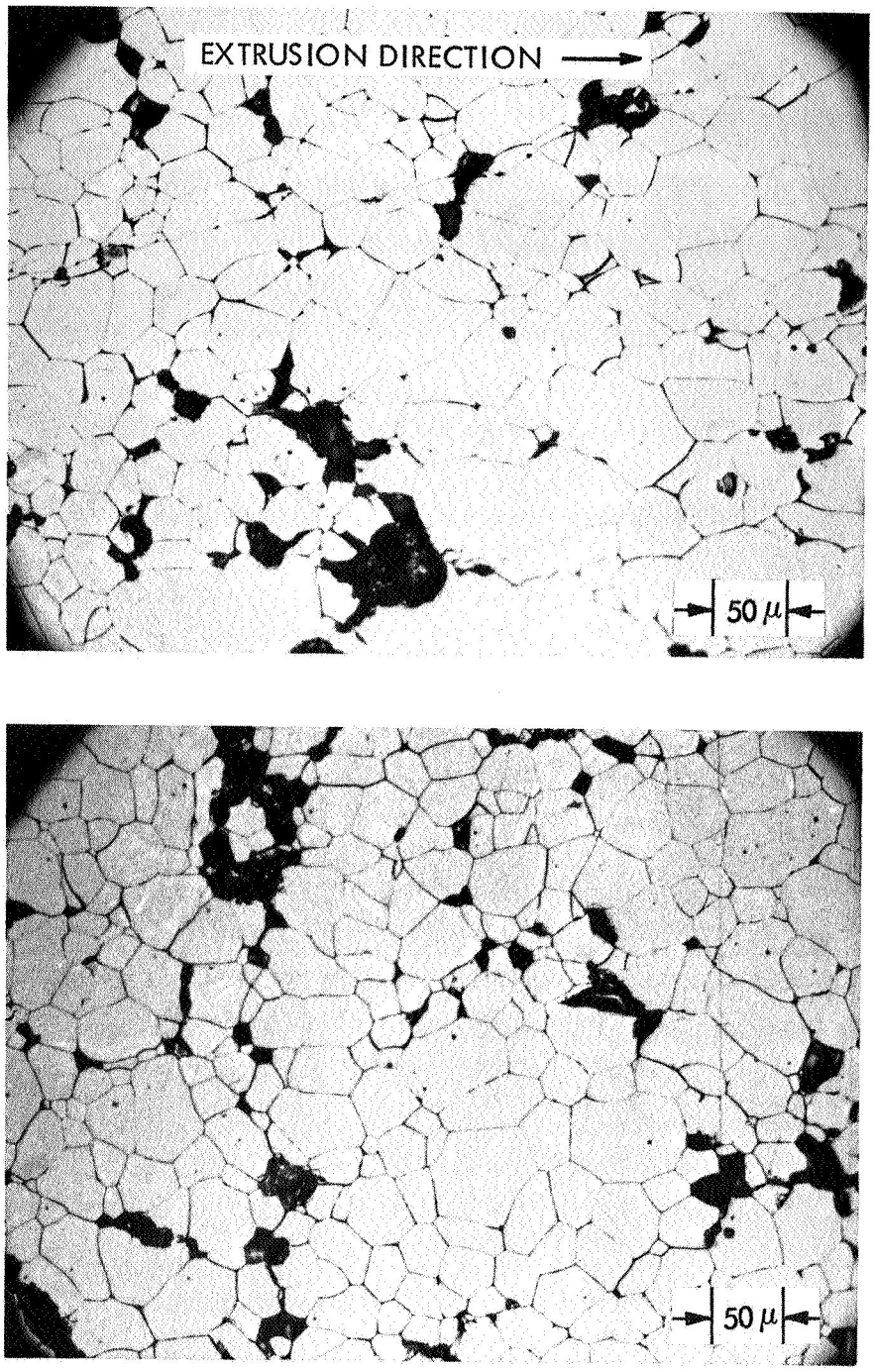

FIGURE 7. EXTRUDED ZrO_2 MICROSTRUCTURE. MATERIAL ZIRCOA C, PARTIALLY STABILIZED WITH 2.9% CaO. BILLET Z-1-3, EXTRUSION MgO-12. HEATED TO APPROXIMATELY 2200°C (OPTICAL PYROMETER READING). (A) LONGITUDINAL, (B) TRANSVERSE SECTIONS.

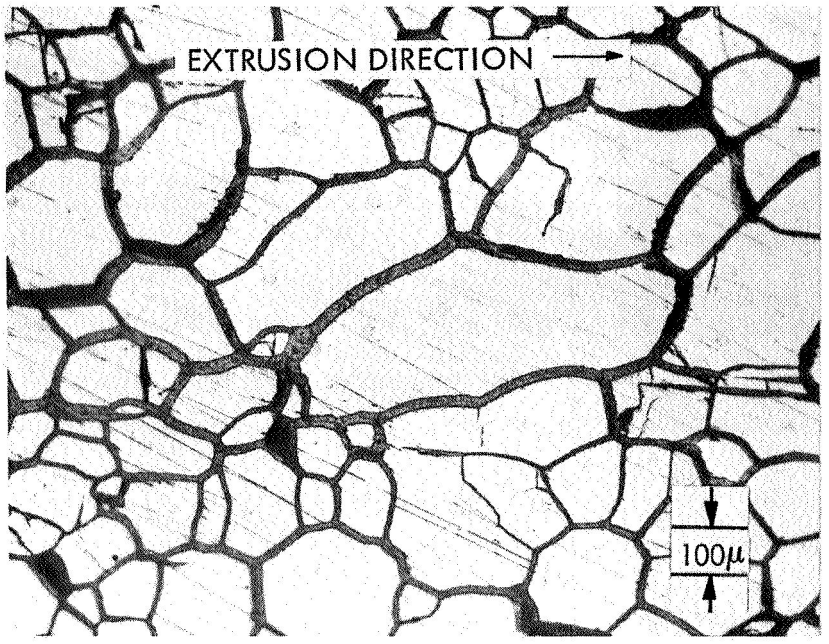

A

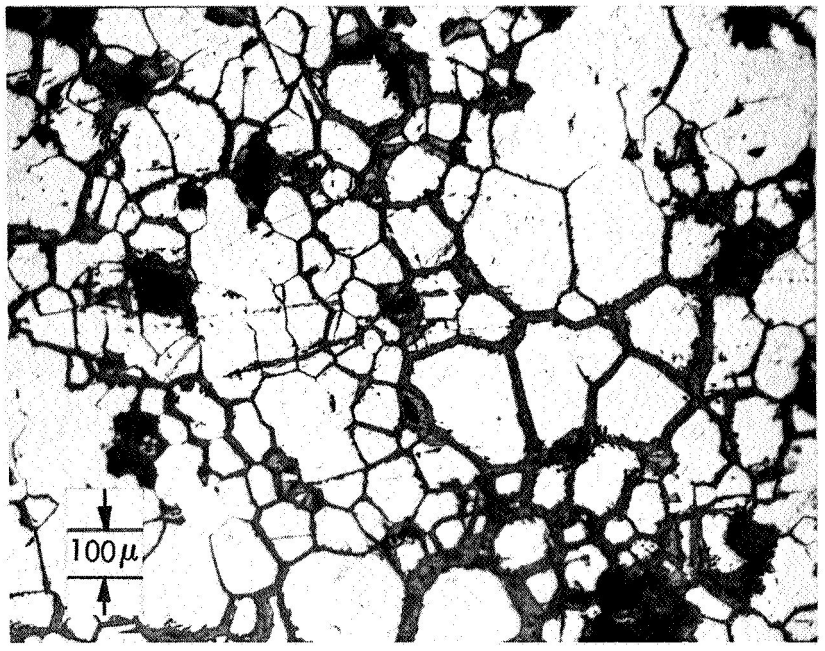

B

FIGURE 8 EXTRUDED MICROSTRUCTURE OF FORGED CaO- BILLET CcF-1-4, EXTRUSION MgO-26 HEATED TO APPROXIMATELY 2000°C (THERMOCOUPLE READING, OPTICAL PYROMETER READING WAS ABOUT 1830°C). (A) LONGITUDINAL, (B) TRANSVERSE SECTIONS.

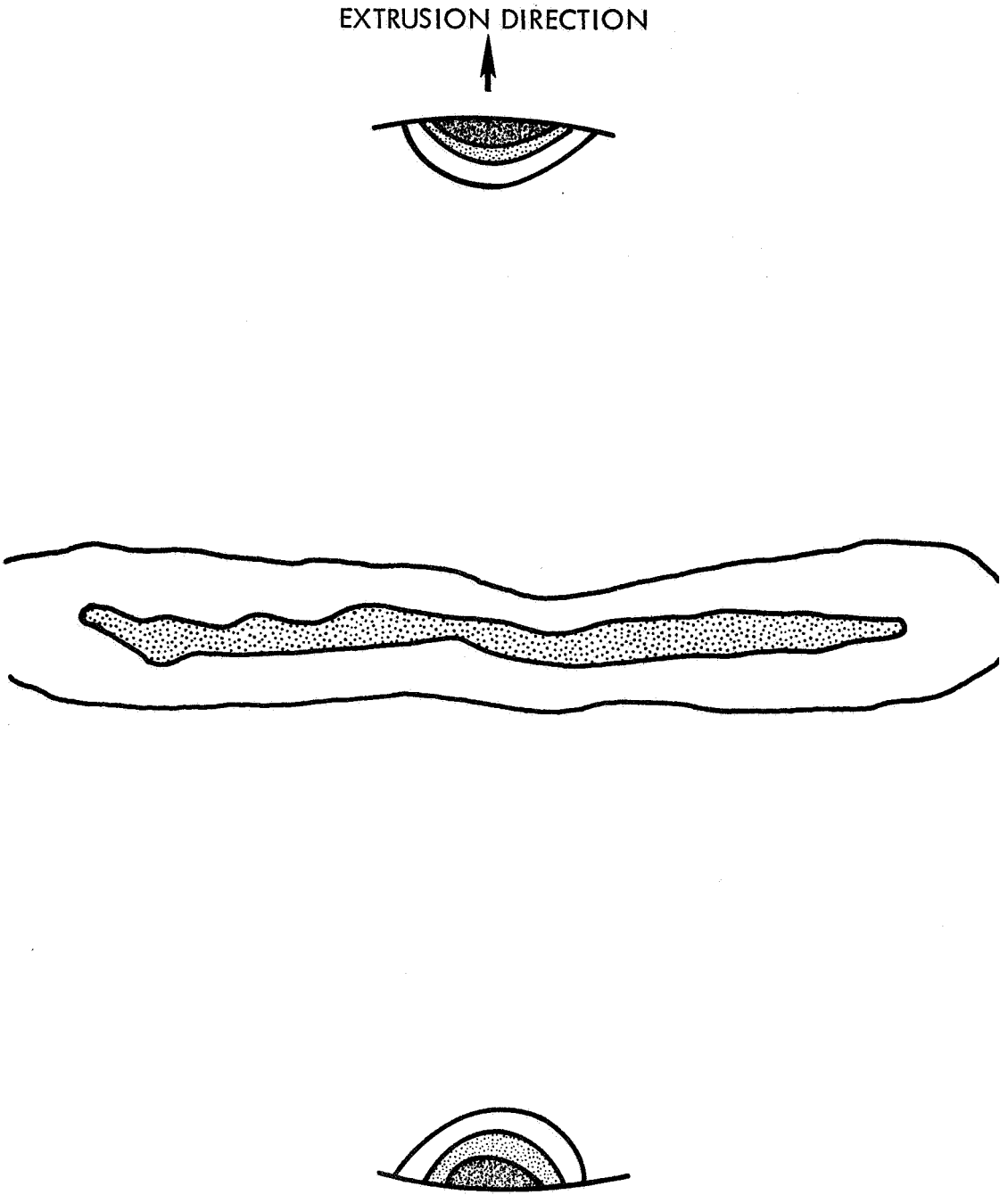

FIGURE 9. (200) POLE FIGURE OF HOT PRESSED AND FIRED MgO BILLET M-4-7 (EXTRUSION MgO-22)

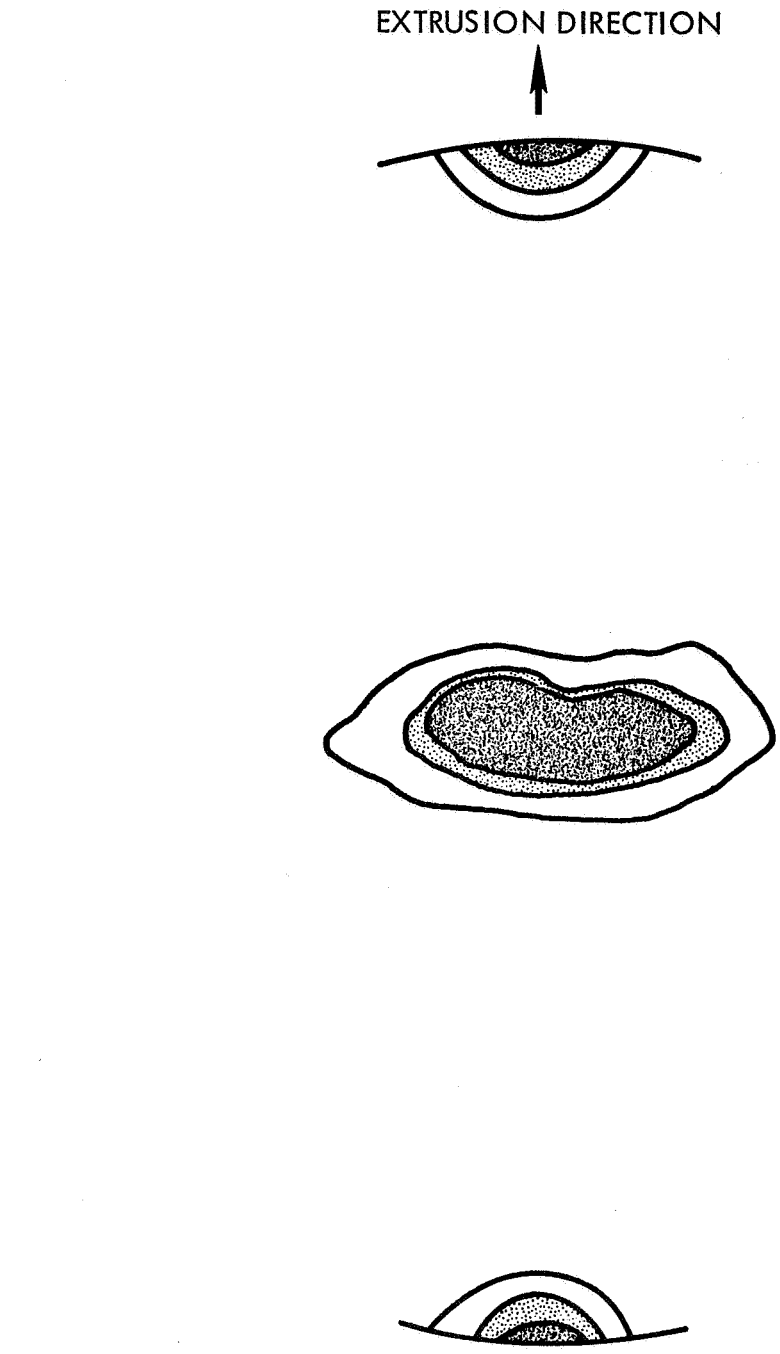

FIGURE 10. (200) POLE FIGURE OF FUSED MgO BILLET M-f-11 (EXTRUSION MgO-18)

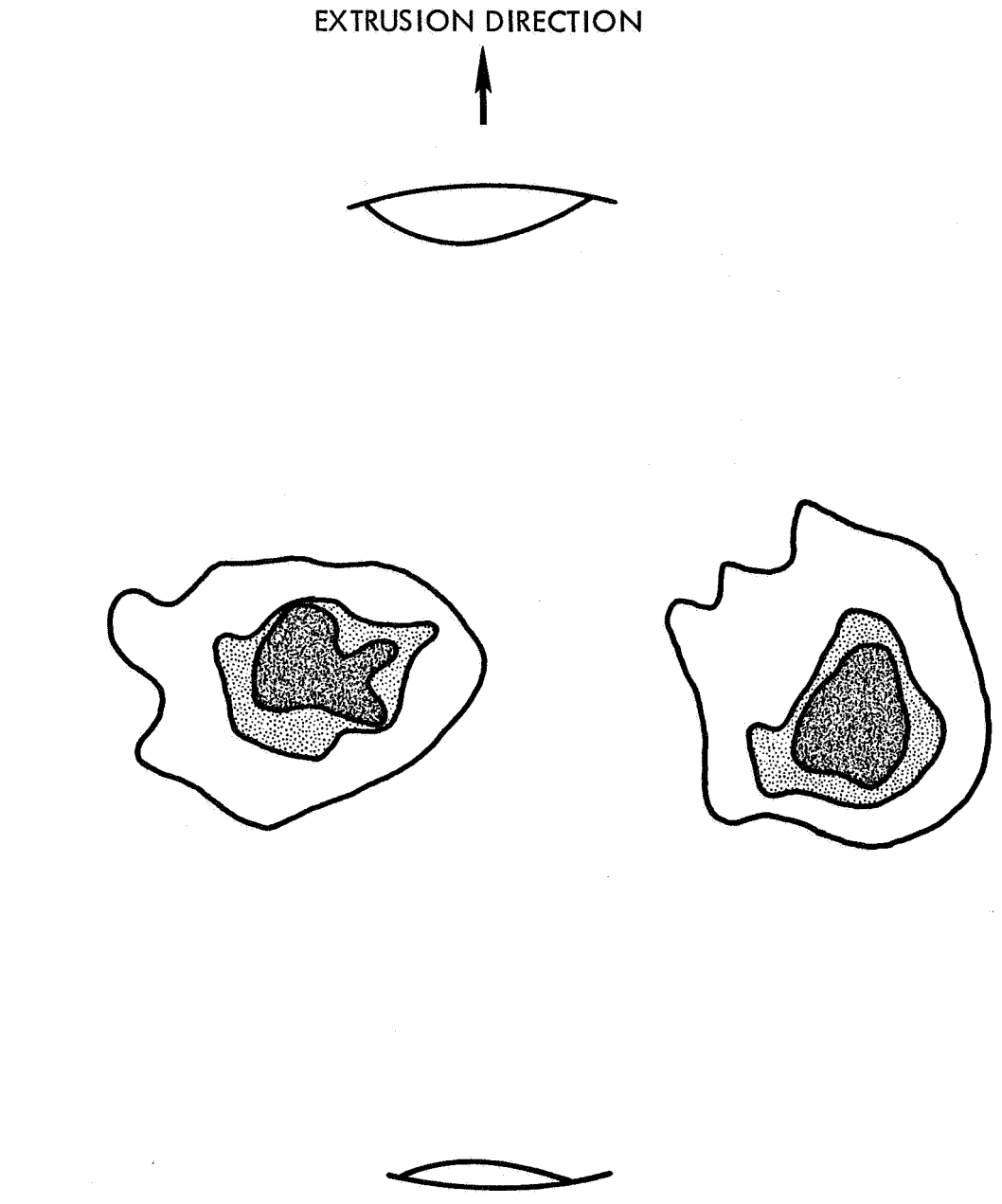

FIGURE 11. (200) POLE FIGURE OF FUSED MgO BILLET M-f-3 (EXTRUSION MgO-3)

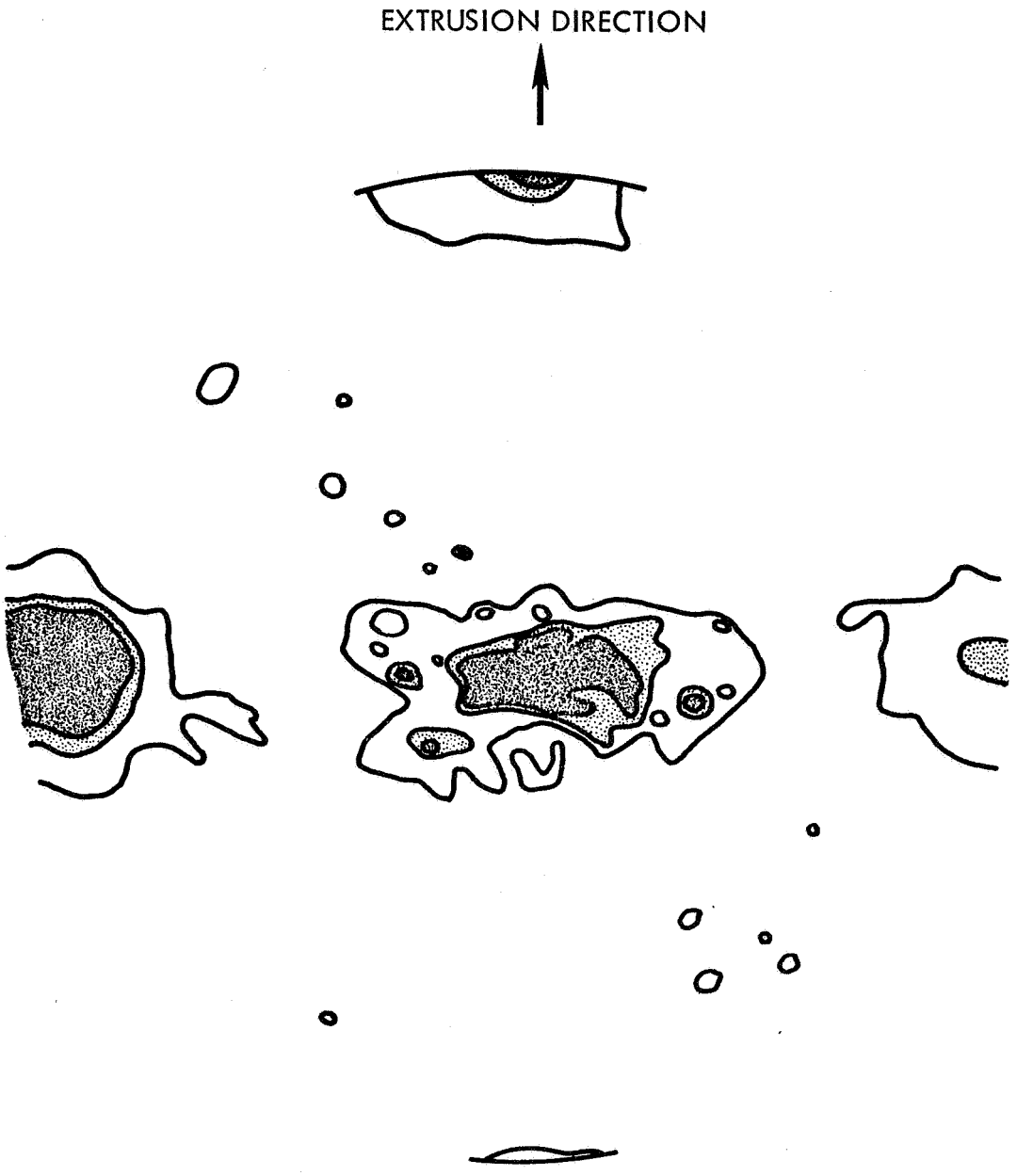

FIGURE 12. (200) POLE FIGURE OF FUSED MgO BILLET M-f-14 (EXTRUSION MgO-22)

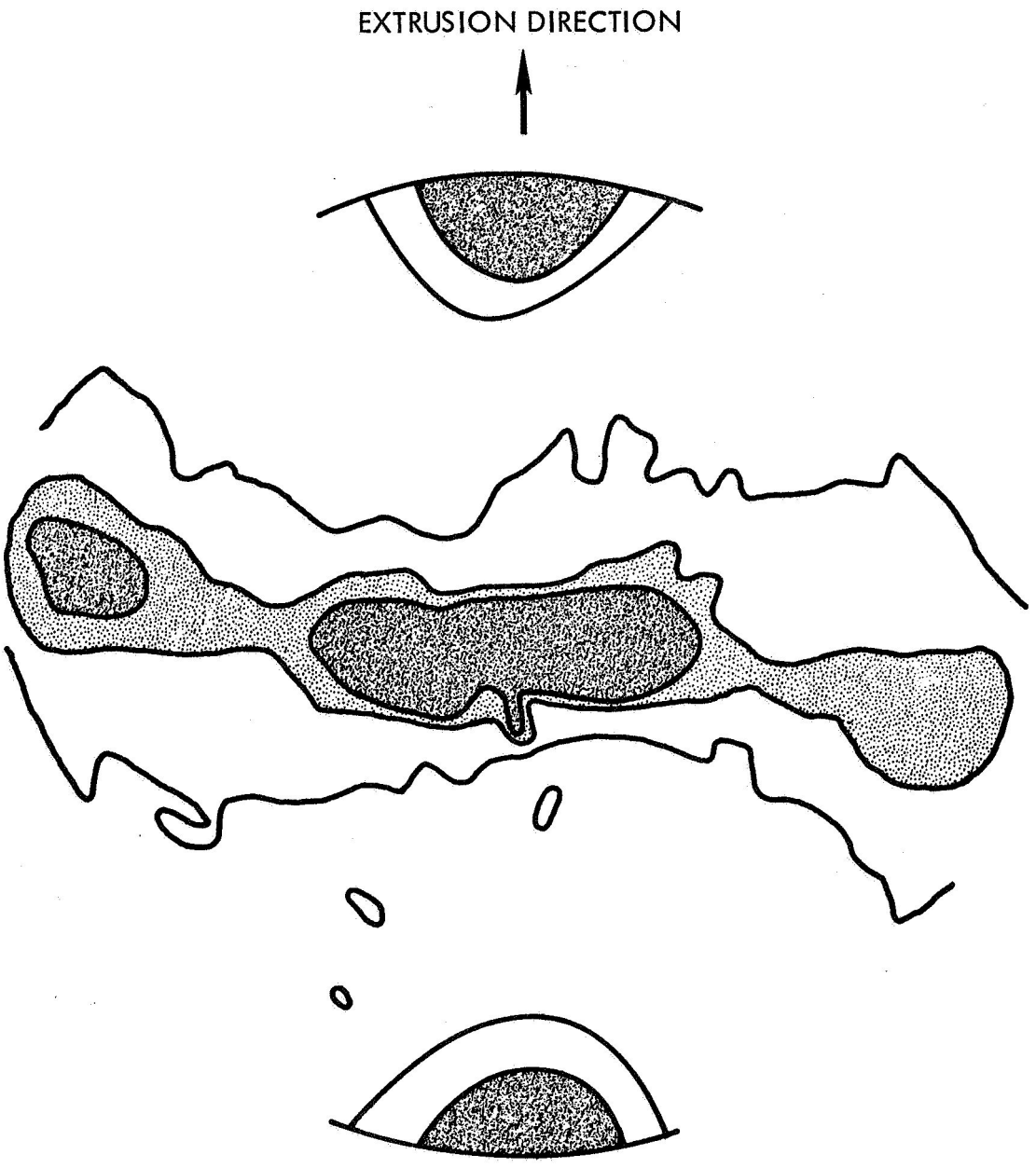

FIGURE 13. (200) POLE FIGURE OF FORGED-EXTRUDED CaO FUSED BILLET CcF-1-4 (EXTRUSION MgO-26)

APPENDIX 1

BILLET VACUUM HOT PRESSING PROCEDURE B (WITHOUT LiF)

1. Powder is directly loaded into the die from sealed bottles, without any prior milling unless milling was previously used to mix alloy agents. Pyrolytic graphite spacers are used between the rams and the specimen when graphite dies are used.

2. The powder is cold pressed at 1000-2000 psi.

3. The die is placed in the vacuum hot press which is pumped down to a chamber pressure of 10^{-4} to 10^{-5} torr in about one hour.

4. After at least 2 hours at 10^{-4}-10^{-5} torr the die is heated to 1650°F(900°C) in about 30 minutes. Temperatures are measured optically at the approximate center of the side of the die.

5. Starting at 1750°F(950°C) the ram pressure is built up to 5000 psi over a period of about 2 minutes.

6. A temperature of 2400°F(1315°C) is then reached in about 20 minutes, while maintaining the ram pressure at 5000 psi.

7. Pressing conditions of 2400°F and 5000 psi are held for 15 minutes with vacuum chamber pressure averaging about 10^{-2}torr.

8. The induction heating power is shut off and the ram pressure released over a period of about 1 minute.

9. The die is removed from the vacuum hot press after cooling for two to four hours.

10. The specimen is ejected from the die at a temperature of 750°F(400°C) or less.